Combined Effects of Terrestrial Diffraction and Ionospheric Reflection on Medium-Frequency Sky-Wave Propagation

Akira KINASE

Abstract

A theoretical analysis is made on the titled subject as an extension of the classical theory (elaborated by H. Bremmer) of the ionospheric propagation. A physical parameter, which is akin to the conventional convergence or divergence coefficient introduced by Bremmer, is formulated in a highly approximate integral representation applicable at low to negative angles of departure/arrival, and the integral is evaluated by numerical means. Part of the result obtained from this analysis is further applied to the estimation of the interhop polarisation coupling factor, which has been formulated by G.J. Phillips and P. Knight. Striking features emerging from, and the adequacy of the present analysis are demonstrated with a typical example.

LIST OF PRINCIPAL SYMBOLS

(r, θ, ϕ) = Spherical coordinates of point of observation.
$\Pi_{sk,p}$ = Sky-wave term for p-hop wave, $(r\Pi_{sk,p}, 0, 0)$ being the radial Hertzian vector.
a = Earth's radius, 6,371 *km*.
L = Geometrical length of ray-hop path from transmitting to receiving point.
ψ = Angle of departure/arrival ($\psi \geq 0$) or angle of diffraction ($\psi < 0$).
$\tau(r)$ = Angle which a radio ray-path makes with a radial direction at a height of $r-a$.
h' = Virtual height of the ionosphere.
ϕ = Semi-vertex angle at $r=a+h'$ of triangulated path.
f = Frequency of an electromagnetic (e.m.) wave radiated from a transmitting aerial.
λ = Wavelength in free space ef an e.m. wave. 〃 〃 〃
$k = 2\pi/\lambda$ = Propagation coefficient in free space.
κ_e = Specific electric permittivity of the ground, rel. free space.
σ = Electric conductivity of the ground.
$\varepsilon_c = \kappa_e - j60\lambda\sigma$ = Complex relative permittivity of the ground.
$\mu(r)$ = Refractive indes of the atmosphere at a height of r-a.
f_p = Critical frequency of the ionosphere.
R, R_v/R_h = Spherical reflection coefficient for vertically/horizontally polarised wave at the earth's surface.
A, C = Convergence or divergence coefficient.
F = Power polarisation coupling factor.
$M_{a,b}$ = Axial ratio of polarisation ellipse, suffices a and b denoting a pair of mutually coupling modes, resp.
$\psi_{a.b}$ = Orientation of polarisation ellipse, suffices denoting quite similary to before.
$\Gamma_{v,h}$ = Multiplying factor for linear component of an elliptically polarised wave,

An extended summary of this article appears in pp. 1125–1126 of PROC. IEE., Vol. 124, No. 12, DECEMBER 1977, and a photocopy of the complete manuscript is deposited in the IEE Library. This paper is a reproduction, but, in a revised form, of the manuscript just referred to.
Received October 22, 1979

suffices v and h denotong vertically and horizontally polarised components resp.

S.I. unit system is used and a time factor exp $(j2\pi ft)$, t denoting time, is suppressed throughout.

1 Introduction

This paper deals with two problems of propagation gain or loss at medium frequency (m.f.) over long distances, namely

(*b*) the contribution due to what may be termed 'convergence gain' or 'diffraction loss, depending upon a given path geometry

(*a*) the contribution due to what may be termed 'inter-hop polarisation coupling loss'.

These problems were taken up by the author as the one yet to be solved in his attempt† of deriving on a theoretical basis a generalised prediction method for night-time m.f. sky-wave field-strengths. Since various pieces of information related to the problems can be referred to in existing text-books and publsihed papers, a brief mention of the physical nature of and the previous work on the problems will be made and followed by the author's comment in order to assist in a better understanding of the orientation of this paper.

As is discussed in detail in the textbook of Bremmer[2], ray-path convergence or focusing, sometimes known as 'ionospheric focusing' or 'horizon focusing', takes place in general for an electromagnetic (e.m.) wave energy transmitted via the ionosphere and the earth's surface and at low angles of departure/arrival. This type of convergence is introduced as a combined effect of the convergence and the divergence which a bundle of radio-rays proceeding along a ray-hop (or wave-hop) path undergo at the reflections against the (lower part of the) ionosphere and the earth's surface respectively, the divergence being excelled by the convergence, and plays a role of significantly modifying the simple inverse-distance attenuation of the field-strength produced by a transmission of an e.m. energy in free space. Under the assumptions that the earth's surface is smooth spherical and the ionosphere is stratified concentrically with the earth's surface and under an additional assumption that a given transmitting and receiving points are situated on the earth's surface, a basic and generalised formula representing the effect of the convergence or divergence has been derived by Bremmer[2] as

$$C=\frac{L}{a}\sqrt{\frac{\cot\psi}{\sin\theta}\left|\frac{\partial\psi}{\partial\theta}\right|} \qquad \text{(see Fig. 1)} \tag{1}$$

Computations of the convergence or divergence coefficient have been made on the basis of eqn. 1 or a modified form of the equation for several types of ionospheric layer models with a specific profile of electron number density, and the results have been applied to an estimation of the sky-wave field-strength. As are illustrated in Figs. 66 and 71 in Reference 2 for a

† This attempt was invoked by 'a series of long-distance propagation measurements in Band 6 (m.f.)'[1], which were conducted during the period 1971 through 1975 as part of the activities of the A.B.U. (Asian Broadcasting Union), and in which the author was entrusted throughout the period to coordinate the whole work related to the measurements and analyse the data collected therefrom.

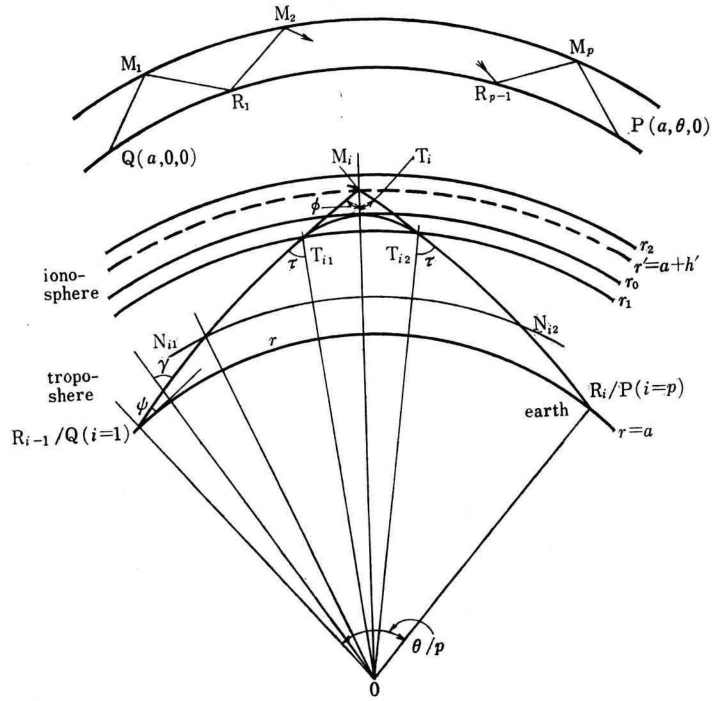

Fig. 1 *Ray-path geometry and parameters or the wave-hop propagation via the ionosphere*
The effect of tropospheric refraction is neglected in the top figure.

sharply bounded layer at low-frequency (l.f.) and for a parabolic layer at high-frequency (h. f.) respectively, the value of C based on eqn. 1 increases with a progressive rapidity as the angle ψ decreases below about 1°, tending to infinity as ψ tends to zero, whichever model mentioned above is used. On the other hand, another factor $|1+R|^2$, which appears in the formula representing the field-strength, and where R denotes the Fresnel reflection coefficient at a flat earth's surface, decreases with a more pronounced rapidity as compared with C over the same range of angles ψ as before. As a consequence, an infinite field-strength is prevented from being realised. It is readily verified that, so far as the earth-to-ionosphere space is assumed homogeneous or inhomogeneous, but, occupied with the standard or a like atmosphere, eqn. 1 leads always to $C\rightarrow\infty$ for $\psi\rightarrow 0$. The occurrence itself of $C\rightarrow\infty$ for $\psi\rightarrow 0$ based on eqn. 1 has been taken up as an annoying problem by a few authors[3,6], and as a result a solution has been provided that a roughness in the ionosphere prevents C from tending to infinity. Among these workers, Bradley[6], in his analysis of the effect of the roughness, used a limiting value of 9 dB for the focusing gain: $G=20\log_{10}$ [convergence coefficient] at $\psi=0$ and for a single hop path. The value 9 dB is quoted in Reference 6 as the one deduced by Pigott. The results from Bradley's work were incorporated by Knight[4] in his theoretical prediction method (wave-hop method) for sky-wave field-strengths at m.f. It should be reminded at this juncture that eqn. 1 has been derived from the second-order approximation for the 'sky-wave term $\Pi_{sk,p}$†', where p is a number of ray-hops, or from a treatment using a simple ray-path model. However, the second-order approximation or the treatment in terms of ray-paths for $\Pi_{sk,p}$, is ruled out when the angle of departure/arrival ψ is less than a certain limiting angle ψ_s††, whether the ionosphere is replaced by a sharply bounded homogeneous layer or a slowly varying stratified layer. Accordingly, for $\psi < \psi_s$, use of C given by eqn. 1 and R (Fresnel reflection coefficient) is invalidated. The situation is quite similar to that encountered in the ground-wave propagation in which a receiving point is situated close to or below the horizon of a transmitting point. Even if the occurrence of $C \to \infty$ for $\psi \to 0$ is avoided by a contribution due to a roughness or some other physical property of the ionosphere, the vanishing of an infinite field strength may turn out to be merely formal if substantially a purely ray-theoretical treatment of the influence of the earth is retained, and a more sophisticated analysis of the problem concerned remains to be made. The above consideration leads to a conclusion that, for $\psi < \psi_s$, the influence of the curved earth's surface and the curved ionospheric layer should be discussed as a combined effect of the terrestrial diffraction and the ionospheric convergence by incorporating a wave-theoretical treatment. The present paper is directed to this goal.

In parallel with the ray-path convergence that has been the topic of the foregoing paragraph, another physical phenomenon of 'polarisation coupling' takes place in the ionosphere. This phenomenon arises because a wave incident on the ionosphere will excite the characteristic modes, ordinary (0) and extraordinary (X), to a degree depending upon how the polarisation of an incident wave resembles that of the respective characteristic mode, and plays an important role in the sky-wave propagation, at m.f. in particular. For a sharply bounded ionospheric layer (homogeneous and anisotropic), an analytic solution based on a full-wave theory for the phenomenon is readily available from a number of pieces of work perfomed by Johler-Walters[10], Sheddy[11] et al. However, for a continuously varying layer (inhomogeneous and anisotropic), a solution comparable to the aforesaid one is yet to be worked out. Instead, a solution based on a simple ray theory has been provided in a compact analytic form by Phillips and Knight[8]. At very oblique angles of incidence, a ray theoretical treatment of the propagation in the ionosphere is of limited accuracy at frequencies in the lower m.f. band, say at frequencies less than about 0.7 MHz. However, since this paper is concerned with another aspect that appears to have been overlooked in the treatment of Phillips and Knight, the discussion on the polarisation coupling is made on the basis of a ray-path model similarly to these authors and as an extension of their work. Reproducing their result from Reference 8, the effect of polarisation coupling is represented generally by a single formula:

$$F = \frac{\begin{aligned} |\Gamma_v(\cos\psi_a + jM_a\sin\psi_a)(\cos\psi_b - jM_b\sin\psi_b) \\ + \Gamma_h(\sin\psi_a - jM_a\cos\psi_a)(\sin\psi_b + jM_b\cos\psi_b)|^2 \end{aligned}}{(1+M_b^2)(1+M_b^2)} \tag{2}$$

† *After Bremmer*, $\Pi_{sk,p}$ replacing $\Pi_j|_{j=p}$ in page 157 in Reference 2.

†† $\psi_s = O[(\lambda/\pi a)^{1/3}]$, a result derived by the present author.

where minor changes in symbols from eqn. 6 of Reference 8 have been made. As is described in Reference 8, this formula is applicable to conditions under which the collision-frequency of electrons remain low at each level of appreciable ionisation, namely Z=(collision frequency ν)/$2\pi\times$ working frequency f)$\ll 1$. These conditions are satisfied in practice at m.f. and at all magnetic latitudes during the night. In what follows only the coupling to the ordinary-wave mode is considered, since the extraordinary-wave mode is heavily absorbed in the ionosphere. As is also described in Reference 8, from eqn. 2 it is inferred that there exist several cases in which a serious reduction of the sky-wave field-strength at a long distance may take place. These cases are enumerated in the same reference, and a satisfactory agreement between experimental results and the computed results based on eqn. 1 (Reference 8), to which eqn. 2 is formally reduced if Γ_v and Γ_h are put equal to unity, is demonstrated in Fig. 7 in the reference for a (geomagnetic) E-W path. The present paper is concerned exclusively with another unfavourable case among the ones referred to above, namely the case in which an intermediate reflection against a sea surface is involved in an N-S multihop path and at very low angles of departure/arrival in particular. That is to say, the effect of polarisation coupling between a wave emerging from the ionosphere at T_{i2} (see Fig. 1) and re-entering at $T_{i+1,1}$ after being reflected from a sea at R_i and the 0-mode of wave at $T_{i+1,1}$, the wave-hop path being oriented along or close to the N-S direction, is of primary interest. This type of polarisation coupling is termed 'inter-hop polarisation coupling' in this paper. In such case, computed results based on eqn. 2 with Γ_v and Γ_h equated to $+1$ and -1, respectively, will in general lead to a very large inter-hop polarisation coupling loss, F equalling zero exactly when $M_a=M_b=-1$ (for the righthanded circular polarisation)[7]. The above approximation of $\Gamma_v=+1$ and $\Gamma_h=-1$ is guided by a geometric-optical concept of planar-specular reflection at a sea surface, and has been used in Reference 8 and elsewhere. A large polarisation coupling loss based on eqn. 2, however, appears to be contradictory to the fact that a higher field-strength has been observed in general over an N-S path and at a long distance such as has been demonstrated by the familiar N-S Cairo curve[1]. This apparent contradiction was confirmed definitely by a comparison between the computed results of F based on eqn. 2 and the directly measured field-strengths on the N-S paths: Akita, Japan — Darwin (5,890 km), Brisbane (7,890 km) and Melbourne (8,645 km), Australia, which were chosen for the regular measurements of the A.B.U.[1] (see the footnote in page 60) and are fully or mostly oversea paths. In face of this fact, a conclusion reached by the author was that, at low angles of departure/arrival, the ray-theoretical treatment of the ground effect, namely the approximation of Γ_v and Γ_h by the Fresnel reflection coefficients, should be replaced by a wave-theoretical treatment. The conclusion was reached by a reasoning entirely similar to that made in the previous problem of ray-path convergence, and by wave-theoretical treatment is meant that of the terresitral diffraction. The present paper is directed also to this goal.

The analysis made in this paper is really an extension of Bremmer's work on the skywave propagation, and is guided intrinsically by a concept akin to a geometric-optical one. With a similar type of idealisation to that which has been stated above for the media influencing

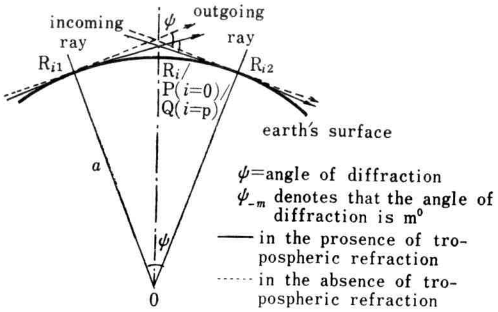

Fig. 2 *Ray-path geometry near intermediate/terminal diffraction segment around the earth's surface*

the sky-wave propagation, the mathematical manipulation starts from an integral representation for the sky-wave term $\Pi_{sk,p}$. This function is then transformed into an approximate integral representation, which may be called a modified form of the one appearing in the second-order approximation for $\Pi_{sk,p}$, and finally evaluated by numerical means. This mathematical procedure makes a break-through to an extreme complexity inherent to a rigorous procedure of summing up the residue series and to an ensuing impracticability of the residue method. The computations are confined to cases in which the W.K.B. approximation or the discussion based on a ray-path model is justified for the propagation in the ionosphere, and are made up to six-hop paths over a range of angles of departure/arrival $|\psi|$ less than a few degrees centred on $\psi=0$, negative angles denoting an angle of diffraction as shown in Fig. 2. As regards the propagation in the earth-ionosphere space, two cases are considered in which the effect of the tropospheric refraction is neglected and that due to an average state of the atmosphere surrounding the earth is allowed for. The coefficient A, which represents a combined effect of the terrestrial diffraction, tropospheric refraction and the ionospheric reflection, is readily evaluated from the final result for $\Gamma_{sk,p}$. This coefficient corresponds to a product: $\frac{1}{2}C\cdot(1+R_Q)(1+R_P)\prod_{i=1}^{p-1}R_i$, which applies for $\psi>\psi_s$ and in which ψ is given by eqn. 1 and R_Q, R_P and R_i represent the ground reflection coefficient R at Q, P and R_i respectively. On the other hand, the ratio Π_h/Π_v is obtained in terms of amplitude and phase as part of the result from the computations for $\Pi_{sk,p}$, namely $\Pi_{sk,p}$ with $p=2$. This result is then used for approximately evaluating the relative value of $F=$[eqn. 2 with $\Gamma_v\to1$† and $\Gamma_h\to\Gamma_h/\Gamma_v$]$=F_{rel}$. Some typical examples of computed results show clearly that A—∞ never takes place even in the absence of roughness in the ionosphere and that a simple approximation of $\Gamma_v=+1$ is inadequate for estimating F on the basis of eqn. 2 when an intermediate ground reflection takes place on a sea. In Table 1 it is demonstrated that a satisfactory agreement between a computed and measured field-strength, the latter being a long-term median value, is obtained when the result from

† This relation is used merely as a reference for estimating the value of Γ_h.

the present analysis has been incorporated in the computation for an N-S multi-hop oversea path.

Several kinds of approximation are used in the analysis of the present problems, and an adequacy of each kind of approximation will be made clear during the discussion.

2 Basis of analysis on the convergence or divergence gain

In this section, the problem is treated by the use of a Hertzian vector $r\Pi_{sk,p}$ as has been done by Bremmer[2]. Since the ionosphere is anisotropic because of the superimposition of the earth's magnetic field on an ionised medium, the simple treatment of using a single vector function $r\Pi_{sk,p}$ is not applicable to the determination of the components of an e.m. field in the earth-ionosphere space even when all media contributing to the propagation are assumed radially symmetrical. However, so far as the present problem is concerned, the treatment is justified to an adequate degree of accuracy because a deviation of a ray-path in the presence of from a one in the absence of the earth's magnetic field turns out to be negligible for the ionosphere (E-layer) met in practice. This aspect has been confirmed by a number of numerically computed results using various model E-layers.

2.1 Integral representation of sky-wave term $\Pi_{sk,p}$ — basic form after Bremmer[2]

In addition to the idealisation, such as has been stated in the previous section, of the media contributing to the propagation, an e.m. wave is assumed to be radiated from a vertical (radially directed) electric dipole which is situated at a terminal point Q. Furthermore, the troposphere is in general assumed stratified concentrically with the earth's surface, the stratification being such as may not cause a turning-back of a ray-path in the troposphere. Using the model that has been mentioned above and a spherical coordinate system (r, θ, φ) with origin at the earth's centre (see Fig. 1), neglecting the earth's magnetic field in the ionosphere, and assuming for a meanwhile that the earth is homogeneous, a function $r\Pi_{sk,tot}$ is identified with the radial Hertzian vector $(r\Pi_{sk,tot}, 0, 0)$† in the space $a \leq r < r_2$ for an e.m. wave radiated from Q and propagated between the earth's surface and the (lower part of the) ionosphere. Then, proceeding quite similarly to Reference 2, $\Pi_{sk,tot}$ is splitted into the sky-wave terms $\Pi_{sk,p}$, the individual sky-wave term $\Pi_{sk,p}$ representing the contribution to $\Pi_{sk,tot}$ of a wave that has gone p times to and fro between the earth's surface and the ionosphere. $\Pi_{sk,p}$ is first developed as an infinite series sum of zonal harmonics and secondly represented by the following complex integral with the aid of Watson transformation:

$$\Pi_{sk,p} = \frac{j}{2}\int_{-\infty-j\delta}^{\infty-j\delta} \frac{n}{\cos(n\pi)}\, g_{sk,p}\left(n-\frac{1}{2}\right) P_{n-1/2}[\cos(\pi-\theta)]\, dn$$

$$\delta \gtrsim 0,\ \delta < |Im\,[k_1 a]| \qquad (3)††$$

† The Hertzian vector for the total field consists of a sum of the ground-wave term $r\Pi_G$ and the total sky-wave term $r\Pi_{sk,tot}$, the latter being concerned exclusively in the present work.

†† The Π-function for the primary field is represented by $\Pi_{prim} = \exp(-jk_1D)/(-jk_1D)$ inside the thin spherical skin with radii $r=b-\Delta$ and $r=b+\Delta(\Delta \gtrsim 0)$, where b and r are the radial coordinates of Q and P resp., $k(r)$ equalling k_1 inside the skin and D denoting the distance $\overline{QP}$.

where $P_{n-1/2}(z)$ is the Legendre function and $g_{sk,p}\ (n-1/2)$ is an even function of n, and is given by

$$g_{sk,p}(\nu)=[1+R(\nu)]^2[R(\nu)]^{p-1}\frac{[u_\nu^{(1)}(a)]^{p+1}}{[u_\nu^{(2)}(a)]^{p-1}}\left[T(\nu)\frac{u_\nu^{(2)}(r_1)}{u_\nu^{(1)}(r_1)}\right]^p\Bigg|_{\nu=n-1/2} \tag{4}$$

in which $R(\nu)$ and $T(\nu)$ are the reflection coefficients of the earth and the ionosphere respectively for a spherical wave and are represented explicitly as follows:

$$R(\nu)=\frac{-(1/k_1^2)\Delta[\log\{ru_\nu^{(1)}(r)\}]|_{r=a}+\Omega[\log\{z\zeta_\nu^{(1)}(z)\}]|_{z=k_2a}+q}{(1/k_1^2)\Delta[\log\{ru_\nu^{(2)}(r)\}]|_{r=a}-\Omega[\log\{z\zeta_\nu^{(1)}(z)\}|_{z=k_2a}-q} \tag{5}$$

$$T(\nu)=\frac{\Delta[\log\{ru_\nu^{(2)}(r)\}]-\Delta[\log\{rf_\nu(r)\}]-q_1}{-\Delta[\log\{ru_\nu^{(1)}(r)\}]+\Delta[\log\{rf_\nu(r)\}]+q_1}\Bigg|_{r=r_1} \tag{6}$$

where $k_1=k(r)_{r=a+0}$, $k_2=k(r)|_{r=a-0}$; $\Delta=1/rdr$, $\Omega=1/zdz$; $q=(1/k^2(r)r)\ (dk(r)/dr)|_{r=a+0}$, $q_1=(1/k^2(r)r)\ (dk(r)/dr)|_{r=r_1-0}$, q_1 vanishing when $dk(r)/dr$ is continuous at $r=r_1\cdot\zeta_\nu^{(i)}(z)$, $u_\nu^{(i)}(r)$, i being 1 or 2, and $f_\nu(r)$ are the functions satisfying the radial wave equation: e.g.,

$$\left[\frac{d^2}{dr^2}+\left\{k^2(r)-\frac{n^2-1/4}{r^2}\right\}\right][ru_\nu^{(i)}(r)]=0 \tag{7}$$

and likewise for the functions $\zeta_\nu^{(i)}(z)$ and $f_\nu(r)$, in the space $r\leq a$, $a<r<r_1$ and $r_1\leq r<r_2$ respectively, $\zeta_\nu^{(i)}(z)$ being the spherical Hankel function of the i-th kind and $u_\nu^{(i)}(r)$ equalling $\zeta_\nu^{(i)}(z)$ when the space in question is homogeneous or $k(r)=k$: constant. $f_\nu(r)$ is a linear combination of $v_\nu^{(1)}(r)$ and $v_\nu^{(2)}(r)$, which are similar in nature to $u_\nu^{(1)}(r)$ and $u_\nu^{(2)}(r)$ respectively. In order to transform eqn. 3 into a workable form, approximate representations of the respective functions appearing in the integrand on the right-hand-side (r.h.s.) of the equation should be introduced. Fortunately, since, from the behaviours of the radial wave functions $\zeta_\xi^{(i)}(z)$, $u_\nu^{(i)}(r)$ and $v_\nu^{(i)}(r)$ and from the behaviour of $[1/\cos(n\pi)]P_{n-1/2}[\cos(\pi-\theta)]$, it is concluded that a dominant contribution to the integration comes from a domain $|n|\lesssim k_1a+O(k_1a)^{1/3}$, only the approximate representations applicable to this domain of n are needed to be considered in the succeeding methematical manipulation.

2.2 Approximations for the radial wave functions ($rk(r)\gg 1$)

In the domain in equestion, the W.K.B. approximations for the functions $u_\nu^{(i)}(r)|_{\nu=n-1/2}$, $i=1, 2$, yield

$$\begin{aligned}
u_\nu^{\binom{1}{2}}(r)&=\frac{\exp(\pm j\alpha\mp j\pi/4)}{r\sqrt{k_1}\ [\xi(r)]^{1/4}}, &&\left(-\frac{\pi}{3}\leq\mathrm{Arg}(\xi)<\frac{\pi}{3}\right)\\
u_\nu^{(2)}(r)&=[\text{the same as above}], &&\left(-\pi\leq\mathrm{Arg}(\xi)<-\frac{\pi}{3}\right)\\
u_\nu^{(1)}(r)&=\frac{\exp(-j\alpha+j\pi/4)+\exp(j\alpha-j\pi/4)}{r\sqrt{k_1}\ [\xi(r)]^{1/4}}, &&(\ ''\ ''\ ''\ )
\end{aligned} \tag{8}$$

where
$$\xi(r) = k^2(r) - \frac{n^2 - 1/4}{r^2}, \tag{9}$$

$$\alpha = \int_{r_0}^{r} \sqrt{\xi(r)}\, dr, \quad (Re \sqrt{\cdots} \geq 0) \tag{10}$$

r_0 being the zero point for $\xi(r)$ of the first-order, and

$$|\omega(r)| = |3\xi'^2/4\xi^2 - \xi''/2\xi| \ll 1, \ ' \text{ denating } d/dr,$$

has been assumed.

When $|\xi(r)| \ll 1$, eqn. 8 does not apply. Then, if $\xi(r)$ is assumed as varying linearly with r,

$$u_{\nu}^{(1)\atop(2)}(r) = \exp(\pm j\pi/6) \sqrt{\frac{\pi\xi}{3k_1 r^2 \xi'}}\ H_{1/3}^{(1)\atop(2)}\left[\frac{2}{3\xi'}\xi^{3/2}\right] \tag{11}$$ [12]

The approximations for $H_n^{(i)}(z)$ have been derived extensively as the second-order and the third-order saddle-point approximations of the integral of Sommerfeld for the functions[9]. The results for $\zeta_{\nu}^{(i)}(z)$ in the doamin concerned of the n-plane are given in the same mathematical form as eqns. 8 and 10 respectively, provided that the following replacements are made:

$$\text{eqn. 9:} \quad \sqrt{\xi(r)} \longrightarrow -jk_1 n/z \cdot \tanh\gamma \tag{9'}$$

$$\text{eqn. 10:} \quad \alpha \longrightarrow -jn(\tanh\gamma - \gamma) \tag{10'}$$

and
$$\xi' \longrightarrow 2k_1/a \tag{12}$$

where $z = k_1 r$, $n/z = \cosh\gamma$, $Re(\gamma)\, Re(\tanh\gamma) \geq 0$, $0 \leq Im(\gamma) < \pi/2$ and $Re(-j\sinh\gamma) \geq 0$, and $|n| \sim k_1 a \gg 1$ has been assumed†.

For a model atmosphere with a familiar linear N-profile, which will be partly used later on, eqn. 9 leads to a simple formal modification of n and a appearing on the r.h.s. of eqns. 9′, 10′, and 12 as follows:

$$n \to n' = Kn, \quad r \to Ka + (r - a), \quad (r/a, \ n/k_2 r \sim 1) \tag{13}$$ ††

where K is the 'effective earth's radius factor'.

The approximations for $v_{\nu}^{(i)}(r)$ are represented in the same form as the first formula in eqn. 8, yielding

$$f_{\nu}(r) = [\text{the same mathematical expression as the r.h.s. of the third formula in eqn. 8}] \tag{14}$$ †††

† According to the third-order saddle-point approximation[9], the variables in the radical and for the Hankel functions on the r.h.s. of eqn. 11 are given by $\pi/6z$ and $n/3\text{-}\tanh^3\gamma\cdot[\exp(-j3\pi/2)]$ respectively, but the difference between this and the present results is insignificant under the condition $n \sim k_1 a \gg 1$.

†† This forms the basis of the conventional 'effective earth's radius method' or 'earth flattening method' employed in the tropospheric propagation.

††† In deriving this equation, the absorption produced at each level of appreciable ionisation has been assumed very low.

On the other hand, $P_{n-1/2}[\cos(\pi-\theta)]$ is represented by the well-known integral of Laplace[2], and, when $|n\sin\theta|\gg 1$, the second-order saddlepoint approximation for the integral yields

$$P_\nu[\cos(\pi-\theta)] = \frac{\exp[jn(\pi-\theta)-j\pi/4]+\exp[-jn(\pi-\theta)+j\pi/4]}{\sqrt{2\pi(n+1/2)\sin\theta}}\Bigg|_{\nu=n-1/2} \tag{15}$$

The restriction $0\leq Im(\gamma)<\pi/2$ confines the range of applicability of eqns. 8 through 14 to a domain in which $\mathrm{Re}(n/z)\geq 0$, but no difficulty is encountered since, when $\mathrm{Re}(n/z)<0$, the approximations for the radial wave functions are given by the same form as these equations multiplied by a constant phase factor respectively.

2.3 The second-order approximation for $\Pi_{sk,p}$

Using eqns. 4 through 15 and expanding $1/\cos(n\pi)$ in ascending power of $[\exp(-jn\pi)]^{2m+1}$, m being a non-negative integer, the individual terms specified by m are finally reduced to a simple integral; e.g.,

$$\Pi_{sk,p}|_{m=0} = \frac{j^{p+1/2}}{k_1 a\sqrt{2\pi\sin\theta}}\int_{n\sim n_s}\frac{\sqrt{n}\,[1+R(\nu)]^2[R(\nu)]^{p-1}}{\sqrt{k_1^2a^2-n^2}}\times$$
$$\exp[-jn\theta-jp\int_a^{r'}\sqrt{k^2(r)-n^2/r^2}\,dr]\,dn \tag{16}$$

which represents the contribution to $\Pi_{sk,tot}$ of a wave that has travelled p times to and fro between the earth's surface and the ionosphere as shown in Fig. 1, and in which n_s has been determined from the principle of stationary phase and is associated with the law of Snellius:

$$n_s = k(r)r\sin\tau(r) = k_1 a\cos\psi = k(r')r'\sin\phi$$
$$= \text{constant along the path from Q to P.} \tag{17}$$

In deriving eqn. 16, $T(\nu)$ given by eqn. 8 has been approximated by

$$T(\nu) = j\exp[-j2\int_{r_1}^{r'}\sqrt{k^2(r)-n^2/r^2}\,dr] \tag{18}$$

The terms $\Pi_{sk,p}|_{m\neq 0}$ can be obtained in a similar form to eqn. 16, however, in practice, at m.f. in particular, the term for $m=0$ becomes the only leading term. $\Pi_{sk,p}|_{m=0}$ alone is therefore considered in the rest of this paper, and the term is denoted by $\Pi_{sk,p}$ for simplicity. Further proceeding similarly to Reference 2, eqn. 16 is reduced to the following compact formula:

$$\Pi_{sk,p} = \Pi_0\cdot C[1+R(\psi)]^2[R(\psi)]^{p-1}[T_c(\phi)]^{p-1} \tag{19}$$

where $\qquad \Pi_0 = \exp(-jk_1\bar{D}_p)/(-jk_1L_p)$

where $\bar{D}_p$ and L_p are the geometric-optical and the geometrical path lengths measured along the entire p-hop trajectory connecting Q with P respectively, C is the same as that given by eqn. 1 with $L_p=L$, and $T_c(\phi)$ is related to $T(\nu)$ as follows:

$$T_c(\phi) = |T(\nu)|^{|T(\nu)|}\big|_{\nu=\nu_S=n_S-1/2} \tag{20}$$

namely the coefficient representing the effect of ionospheric absorption.

When the ionosphere is replaced by a sharply bounded layer, $T_c(\phi)$ is reduced to a coefficient with a similar physical meaning to $R(\psi)$, provided that another reflection of an e.m. wave does not occur in the sapce $r_1 \leq r < r'$:

$$T_c(\phi) = T(\nu_s) \tag{20'}$$

$T(\nu)$ being represented by the same form as eqn. 6 where $f_\nu(r)$ is replaed by $v_\nu^{(2)}(r)$ and the r.h.s./of eqn. 18 being equated to unity.

Now the assumption made at the outset of an homogeneity of the earth can be waived, so far as an homogeneity of the ground around the terminals Q and P and the intermediate reflection points R_i, $i=1,\ldots,p$, is secured to such an extent as a geometric-optical reflection at the ground is permitted. The assumption of homogeneity of the ionosphere may be waived likewise. As a result eqn. 19 can be generalised to the following form:

$$\Pi_{sk,p} = \Pi_0 \cdot C(1+R_Q)(1+R_P) \prod_{i=1}^{p-1} R_i \prod_{i=1}^{p} T_{ci} \tag{19'}$$

where R_Q, R_P and R_i represent $R(\psi)$ at Q, P and R_i, and T_{ci} represents $T_c(\phi)$ at the ionospheric region around T_i, respectively.

Theoretical computations of sky-wave field-strengths have so far been made on the basis of eqn. 19 or 19′. However, the second-order approximation for $\Pi_{sk,p}$ applies only when an e.m. wave is propagated along a well-intervisible path between the earth's surface and the ionosphere. such as between Q and T_{11}, T_{12} and R_1, and so forth. The situation is entirely similar to that encountered in the ground-propagation[2], and when each pair of these points are not well-intervisible, an alternative method for estimating $\Pi_{sk,p}$ should be developed. By 'not well-intervisible' is meant that the angles of departure/arrival ψ are low to negative, a negative ψ implying that each hop-path involves a pair of diffraction segments along the earth's surface as shown in Fig. 2.

From what has been stated so far, it is evident that a substantial contribution to $\Pi_{sk,p}$ at these angles of departure/arrival is made by the integration over a shrot range of n including $n=k_1 a$ along the real n-axis. An analysis for the estimation of $\Pi_{sk,p}$ in question can therefore be made as an extension of the second-order approximation, as is described in the following section.

2.4 Approximations applicable at low to negative angles of departure/arrival for $u_\nu^{(i)}(r)$, $R(\nu)$ and $T(\nu)$

Since, for the propagation at m.f. and at low to negative angles of departure/arrival, the lower atmosphere adjacent to the earth's surface may in practice be highly approximated by a one with a linear N-profile, an approximation for $u_\nu^{(i)}(r)$ for $r \sim a$ can be determined from eqns. 11 through 13, 9′ and 10′:

$$u_\nu^{\binom{1}{2}}(r) = \zeta_\nu^{\binom{1}{2}}(z) = \pm \exp(\mp j\pi/3) \sqrt{\frac{\pi}{6Kz}} \tanh \gamma_a H_{1/3}^{\binom{1}{2}}(\xi) \tag{21}$$

where $\tanh\gamma_a = \sqrt{1-\dfrac{z^2}{n^2}}$, $\xi = \dfrac{Kz}{3}\tanh^3\gamma_a \exp(-j3\pi/2)$

$z = k_1 a$, $\nu = n-1/2$, $\nu' = n'-1/2$ and $n' = kn$.

When the earth-ionosphere space is homogeneous, eqn. 21 applies with K equated to unity.

On the other hand, since an ample space below the lower boundary of the ionosphere, namely the space $a+20$ km (upper boundary of the trosophere) $\lesssim r \lesssim r_1$ (around $a+90$ km), can be regarded as vacuo, $u^{(i)}(r)$ for $r \sim r_1$ is always equated to $\zeta_\nu^{(i)}(z)$. In addition, since the magnitude of $\gamma = \text{arccosh}\ (n/z) \sim \text{arccosh}\ (a/r_1)$ ($\because n \simeq k_1 a$) secures a validity of the second-order saddle-point approximation for $u_\nu^{(i)}(r)$, eqns. 8, 9′ and 10′ lead to

$$u_\nu^{\binom{(1)}{(2)}}(r) = \zeta_\nu^{\binom{(1)}{(2)}}(z) = \frac{\exp[\pm n(\tanh\gamma - \gamma) \mp j\pi/4]}{\sqrt{-jnz\tanh\gamma}} \tag{22}$$

Likewise, the W.K.B. approximation for $\zeta_\nu^{(i)}(r)$ and accordingly $T(\nu)$ given by eqn. 8 and eqn. 18 respectively apply for the space $r_1 \leq r < r'$.

The exponent appearing on the r.h.s. of eqn. 18 has a physical meaning:

$-jk_0P = -jk_1P$, P being the phase path such as from T_{i1} via T_i to T_{i2} in Fig. 1, for a radio-ray with an angle of incidence arcsin $(n/k_0r_1) = \phi(n)$, (23)

and P is related to another physical parameter 'equivalent path' P'[7] = triangulated path such as $\overline{T_{i1}M_i} + \overline{M_iT_{i2}} = 2\overline{T_{il}M_i}$:

$$P = P' + \Delta P \tag{24}$$

where ΔP for a 'parabolic layer is highly approximated by

$$\Delta P = \frac{\Delta r}{\cos\phi(n)}\left[1 - \frac{1}{2}\left(\eta + \frac{1}{\eta}\right)\log\frac{\eta+1}{\eta-1}\right]^{\dagger} \tag{25}$$ [7]

with $\eta = f_p/f\cos\phi(n)$.

In deriving eqn. 25, the curvature of the ionosphere has been neglected. Although a rigorous analytic expression for ΔP for a curved parabolic layer can be derived similarly to the derivation of ϕ such as is described in page 232 in Reference 2, the above approximation meets the practical purpose so far as the reflection from the E-layer is concerned.

Eqns. 4, 18 and 23 through 25 lead to

$$T(\nu)\frac{u_\nu^{(2)}(r_1)}{u_\nu^{(1)}(r_1)} = jT_c(\nu)\exp[-j\Delta P(\nu)]\frac{u_\nu^{(2)}(r')}{u_\nu^{(1)}(r')} \tag{26}$$

where $T_c(\nu) = |T(\nu)|$. [cf. eqn. 20′]

The last term $\zeta_\nu^{(2)}(r')/u_\nu^{(1)}(r')$ appearing on the r.h.s. of eqn. 26 is the same as that which is obtained when the reflection of an e.m. wave takes place at a level of 'virtual height'

† $\Delta r = \bar{r} - r_1 \fallingdotseq (r_2 - r_1)/2$: half thickness of the ionosphere; $\bar{r} = 2r_1r_2/(r_1+r_2)$, r_2 being the upper boundary of the parabolic layer.[2]

$h'=r'-a$. From eqn. 22 this term is approximated by

$$\frac{u_\nu^{(2)}(r')}{u_\nu^{(1)}(r')}=\frac{\zeta_\nu^{(2)}(z)}{\zeta_\nu^{(1)}(z)}=\exp\left[-2n(\tanh\gamma_{h'}-\gamma_{h'})+j\pi/2\right] \tag{27}$$

where $z=k_0r'=k_1r'$ and $\tanh\gamma_{h'}=\sqrt{1-\dfrac{z^2}{n^2}}$.

Substituting from eqn. 21 and eqns. 8 through 10, 9′ and 10′ for $u_{\nu'}^{(i)}(r)$ and $\zeta_{\nu'}^{(i)}(z)$ respectively into eqn. 5,

$$\left.\begin{aligned}
&R(\nu)=\frac{N(\nu')}{M(\nu')}=\frac{\exp(j\pi/6)K\tanh\gamma\,\mathrm{sech}^2\gamma z^{1/3}H_{2/3}^{(1)}(\xi)/H_{1/3}^{(1)}(\xi)-1/\delta}{\exp(-j\pi/6)K\tanh\gamma\,\mathrm{sech}^2\gamma z^{1/3}H_{2/3}^{(2)}(\xi)/H_{1/3}^{(2)}(\xi)+1/\delta},\\
&\qquad\zeta_{\nu'}^{(1)}(z)\zeta_{\nu'}^{(2)}(z)\left[1+R(\nu)\right]=-\frac{j2}{z^2M(\nu')}z^{1/3}\\
&\text{where}\\
&\qquad\delta=\frac{-j\varepsilon_c}{z^{1/3}\sqrt{\varepsilon_c-\cos^2\psi(n)}},\quad(|k_2|\gg k_1,\ Re\sqrt{}\geq 0)
\end{aligned}\right\} \tag{28}$$

z and ξ are the same as those defined in eqn. 21 and q appearing on the r.h.s. of eqn. 5 has been neglected, δ with $\cos^2\psi=1$ being the parameter introduced by Bremmer[2].

From standard textbooks in mathematics are derived the following formulae:

$$H_{1/3}^{\binom{1}{2}}(2x)=\mp j\frac{2}{\sqrt{3}\,\Gamma\left(\frac{2}{3}\right)}x^{-1/3}\left[F_2(x)-c_2\exp(\mp j\pi/3)x^{2/3}F_4(x)\right],$$

$$H_{2/3}^{\binom{1}{2}}(2x)=\mp j\frac{2}{\sqrt{3}\,\Gamma\left(\frac{1}{3}\right)}x^{-2/3}\left[F_1(x)+c_1\exp(\pm j\pi/3)x^{4/3}F_5(x)\right] \tag{29}$$

where $\Gamma(x)$ is the Gamma function,

$$c_1=\Gamma\left(\frac{1}{3}\right)\Big/\Gamma\left(\frac{5}{3}\right)=2.9678\cdots,\quad c_2=\Gamma\left(\frac{2}{3}\right)\Big/\Gamma\left(\frac{4}{3}\right)=\frac{9}{2c_1};$$

$$F_m(x)=1-\frac{3}{1!m}x^2+\frac{3\cdot3}{2!m(m+3)}x^4-\frac{3\cdot3\cdot3}{3!m(m+3)(m+2\cdot3)}x^6+\cdots,$$

$$m=1,2,4\text{ or }5.$$

From eqns. 28 and 29,

$$M(\nu')=M(\xi,K,\delta)=j\exp\left(-j\frac{\pi}{6}\right)K^{2/3}\cdot c_0\left.\frac{F_1(x)+c_1\exp\left(-j\frac{\pi}{3}\right)x^{4/3}F_5(x)}{F_2(x)-c_2\exp\left(j\frac{\pi}{3}\right)x^{2/3}F_4(x)}+\frac{1}{\delta}\right|_{x=\xi/2}$$

$$N(\nu')=N(\xi,K,\delta)=j\exp\left(j\frac{\pi}{6}\right)K^{2/3}\cdot c_0\left.\frac{F_1(x)+c_1\exp\left(j\frac{\pi}{3}\right)x^{4/3}F_5(x)}{F_2(x)-c_2\exp\left(-j\frac{\pi}{3}\right)x^{2/3}F_4(x)}-\frac{1}{\delta}\right|_{x=\xi/2}$$

where $$c_0 = 6^{1/3}\Gamma\left(\frac{2}{3}\right)\Big/\Gamma\left(\frac{1}{3}\right) = 0.9184\cdots \tag{30}$$

and sech $^2\gamma$ has been approximated by unity.

From eqns. 21 and 30,

$$\frac{u_\nu^{(1)}(r)}{u_\nu^{(2)}(r)} = -\exp\left(j\frac{\pi}{3}\right)K_h\left(\frac{\xi}{2}\right), \quad K_h(x) = \left.\frac{F_2(x) - c_2\exp\left(-j\frac{\pi}{3}\right)x^{2/3}F_4(x)}{F_2(x) - c_2\exp\left(j\frac{\pi}{3}\right)x^{2/3}F_4(x)}\right|_{x=\xi/2} \tag{31}$$

Another function $H(\xi, K, \delta)$ is defined for later convenience as follows:

$$H(\xi, K, \delta) = \left[F_2\left(\frac{\xi}{2}\right) - c_2\exp\left(j\frac{\pi}{3}\right)\left(\frac{\xi}{2}\right)^{2/3}F_4\left(\frac{\xi}{2}\right)\right]\cdot M(\xi, K, \delta) \tag{32}$$

2.5 Integral representation of $\Pi_{sk,p}$ — approximate form applicable at low to negative angles of departure/arrival

Following a mathematical procedure similar to that which has been employed in deriving eqn. 16, but, using eqns. 21 through 32 properly, eqn. 3 is transformed into

$$\Pi_{sk,p} = (-)^{2p-1}\exp\left(-j\frac{\pi}{4} + jp\frac{\pi}{3}\right)\frac{3\cdot 6^{1/3}\Gamma^2\left(\frac{2}{3}\right)}{2\pi^2\cdot z^{5/6}}\cdot K^{5/3}\cdot\frac{L_p}{D}\cdot\frac{\sqrt{2\pi\chi}}{-jk_1L_p}\cdot\sqrt{\frac{\theta}{\sin\theta}}\ \times$$
$$\int_{n\sim z} dn\sqrt{n}\ \frac{\left[K_h\left(\frac{\xi}{2}\right)\right]^{p-1}}{H(\xi, K, \delta)_Q\, H(\xi, K, \delta)_P}\prod_{i=1}^{p-1}\left.\frac{N(\xi, K, \delta)}{M(\xi, K, \delta)}\right|_i\cdot[T_c(\nu)]^p\,[\exp\{-j\Delta P(\nu)\}]^p\times$$
$$\exp\left[-jn\theta - 2pn(\tanh\gamma_{h'} - \gamma_{h'})\right] \tag{33}$$

where $D = a\theta$ is the surface distance $\widehat{QP}$ and $\chi = z^{1/3}\theta|_{z=k_1a}$ is a parameter defined by Bremmer[2]. In deriving this equation, an assumption of homogeneity in the earth's electrical properties has been waived in an analogous fashion to the reduction from eqn. 19 to eqn. 19′, the suffices, Q, P and i implying similarly to those appearing in the latter equation.

The angular distance θ is obtained from a purely geometric-optical consideration as follows:

$$\theta = 2pa\cos\psi(n_s)\int_a^{r_M}\frac{dr}{r\sqrt{r^2\mu^2(r) - a^2\cos^2\psi(n_s)}} \quad (\psi \geq 0)^2 \text{ (Ref. eqn. 17)}$$
$$= \quad '' \quad '' \quad '' \quad '' \quad |_{\psi=0} + p|\psi| \qquad (\psi < 0) \tag{34}$$

where $\mu(r)$ is the refractive index of a medium.

If the variable of integration in eqn. 33 is changed from n to t as

$$n = z + \exp(+j\pi)\cdot 6^{2/3}z^{1/3}t/2,$$

ξ in eqn. 21→ $$\xi = 2Kt^{3/2} \quad (n \leq z)$$

$$(n \sim z,\ t \geq 0)$$

$$= \exp\left(-j\frac{3\pi}{2}\right) 2Kt^{3/2} \quad (n > z) \tag{35}$$

and the exponent appearing on the r.h.s. of eqn. 27, to the same order of approximation, is transformed into

$$n(\tanh \gamma_{h'} - \gamma_{h'}) = -n\gamma_{h'}^3/3 = \frac{j}{3}(\chi_{h'}^2 \pm 6^{2/3}t)^{3/2} \quad (n \lessgtr z,\ h' \ll a,$$

with $\chi_{h'} = \sqrt{2h'/a}\ z^{1/3}$ $\qquad Re\sqrt{} \geq 0)$ (36)

$\chi_{h'}$ being another parameter introduced by Bremmer[2].

Substitution from eqns. 35 and 36 into eqn. 33 yields

$$\Pi_{sk,p} = 2\overline{\Pi_0}\, B\, I_p$$

where

$$\overline{\Pi_0} = \exp(-jk_1L_p)/(-jk_1L_p),$$

$$B = -\exp\left(-j\frac{\pi}{4} + jp\frac{\pi}{3}\right)\frac{9\cdot\Gamma^2\left(\frac{2}{3}\right)}{4\pi^2} K^{5/3}\frac{L_p}{D}\sqrt{2\pi\chi}\sqrt{\frac{\theta}{\sin\theta}}$$

$$L_p = a\theta + p\frac{2}{3}\chi_{h'}^3 \fallingdotseq [\text{triangulated path length: } \widehat{QT_1} + \widehat{T_1R_1} + \cdots + \widehat{T_pP}]\dagger \tag{37}$$

$$I_p = \int_0^\infty [U_p^-(t', K, \delta)\exp\{-jf_p^-(t, \chi, \chi_{h'})\}V_p^-(t) \times U_p^+(t', K, \delta)\exp\{-jf_p^+(t, \chi, \chi_{h'})\}V_p^+(t)]dt|_{t'=K^{2/3}t}$$

where

$$f_p^{\mp}(t, \chi, \chi_{h'}) = \mp\frac{6^{3/2}}{2}\chi t + p\frac{2}{3}[(\chi_{h'}^2 \pm 2t)^{3/2} - \chi_{h'}^3] \quad (n \lessgtr z)$$

$$U_p^-(t', K, \delta) = \frac{[K_h(x)]^p}{H(x, K, \delta)_Q\, H(x, K, \delta)_P}\prod_{i=1}^{p-1}\frac{N(x, K, \delta)}{M(x, K, \delta)}\Big|_i\Big|_{x=t'^{3/2}},$$

$$U_p^+(t', K, \delta) = \quad '' \quad '' \quad '' \quad '' \quad '' \quad \Big|_i\Big| x = \exp\left(-j\frac{3\pi}{2}\right)t'^{3/2}$$

$$V_p^{\mp}(t) = [T_c(\nu)]^p[\exp\{-j\Delta P(\nu)\}]^p \text{ for } n \lessgtr z. \tag{38}$$

The above integral forms the basis on which I_p is computed by numerical means. The individual functions M, N, K_h and H comprising the integrand for the integral with respect to t, although represented in an apparently cumbersome form, are well behaved for enabling I_p to be evaluated numerically at and around $n=k_1a$ or $\psi=0$. That is to say,

† An increment in L_p due to the effect of tropospheric refraction has been neglected.

indeed, a mathematical complexity is introduced by the presence of the functions F_m in each of the above-mentioned functions and in addition by a very slow convergence of the series sum at $t'^{3/2}\gtrsim 1.5$, but then an alternative means of the conventional second-order saddle-point approximation for the Hankel functions $H_\nu^{(i)}(z)$, $\nu=1/3,\ 2/3;\ i=1,\ 2$, waives the difficulty in question. For instance, in the range of $n>z$.

$$\text{eqn.. 31 and 35} \to K_h\left(\frac{\xi}{2}\right) = -1+\exp\left(-j\frac{\pi}{3}\right)\frac{F_2(jx)-c_2x^{2/3}F_4(jx)}{F_2(jx)+c_2\exp\left(j\frac{\pi}{3}\right)x^{2/3}F_4(jx)}\Bigg|_{x=t'^{3/2}},$$

but the second term of the r.h.s. of this equation is directly transformed using the Hankel functions alone into

$$\frac{1}{1+\exp\left(-j\frac{\pi}{3}\right)H_{1/3}^{(2)}(jx)\,/\,H_{1/3}^{(1)}(jx)}$$

and

$$K_h(jx)\to -1 \text{ for } x\gtrsim 1.5 \tag{39}$$

is readily derived.
Likewise,

$$\text{eqn. 30} \to \frac{N(\xi,K,\delta)}{M(\xi,K,\delta)} \to -1 \tag{40}$$

and an exponential increase of

$$\text{eqn. 32} \to H(\xi,K,\delta) \text{ for } \xi\gtrsim 3$$

are derived, and as a result a substantial contribution to I_p from the integration over the range $n>z$ is confined to a very short interval of $n-z\gtrsim 2\cdot 6^{2/3}\cdot 1.5\cdot z^{1/3}$.

A contribution to I_p from the range $n\leq z$ can be discussed similarly to before and a similar conclusion is reached as regards the significant range of integration.

3 Combined effect of terrestrial diffraction and ionospheric reflection

3.1 Simplified integral representation of $\Pi_{sk,p}$ by further approximation

To facilitate computations of sky-wave field-strengths at m.f. without losing much rigor, futher simplifications are introduced as regards the electrical properties of the earth. First, the ground at and around the end-points Q and P is assumed perfectly conducting ($|\delta|\to\infty$). This assumption is justified because the effect of a finite ground conductivity at Q and/or P can be allowed for separately and is introduced mainly for the purpose of facilitating a procedure of field-strenght prediction. In Section **5** is used a numerical result of the separate allowance at P by an approximate method. Secondly, out of the $(p-1)$ intermediate reflection points at ground, R_i in Fig. 1, for a p-hop path, m points are assumed situated on a strongly absorbing land ($|\delta|\to 0$) and the remaining $(p-1-m)$ points on a perfectly conducting sea ($|\delta|\to\infty$). This assumption is also justified to a reasonable to a sufficient degree of approximation, $|\delta|\to\infty$ for a sea at m.f. being justified in particular. Then B in eqn. 37 and $U_p^{\pm}(t', K, \delta)$ in eqn. 38 are modified as follows:

$$B = -\exp\left(-j\frac{\pi}{4}\right)\exp\left[j\pi(2p-m)\frac{1}{3}\right]\frac{3\cdot 6^{1/3}\,\Gamma^2\left(\frac{1}{3}\right)}{8\pi^2}\times$$

$$K^{1/3}\frac{L_p}{D}\sqrt{2\pi\chi}\sqrt{\frac{\theta}{\sin\theta}},$$

$$U_p^{\mp}(t', K, \delta)\rightarrow U_p^{\mp}(t') = \frac{1}{[K_{vd}(x)]}[K_v(x)]^{p-1-m}[K_h(x)]^m$$

with $x = t'^{3/2}$ for U_p^- and $\exp\left(-j\frac{3}{2}\pi\right)t'^{3/2}$

for U_p^+, respectively, (41)

where

$$K_v(x) = \frac{F_1(x) + c_1\exp\left(j\frac{\pi}{3}\right)x^{4/3}F_5(x)}{F_1(x) + c_1\exp\left(-j\frac{\pi}{3}\right)x^{4/3}F_5(x)},$$

$$K_{vd}(x) = [\text{denominator of } K_v(x)] \tag{42}$$

$K_v(x)$ behaves similarly to $K_h(x)$ for $x = jt'^{3/2}$ and $|x| \gtrsim 1.5$ (ref. eqn. 39), i.e., for $n > z$

$$K_v\left(\frac{\xi}{2}\right) = -1 + \exp\left(j\frac{\pi}{3}\right)\frac{F_1(jx) - c_1x^{4/3}F_5(jx)}{F_1(jx) + c_1\exp\left(-j\frac{\pi}{3}\right)x^{4/3}F_5(jx)}\Bigg|_{x=t'^{3/2}},$$

$$\left|1 + K_v\left(\frac{\xi}{2}\right)\right| \rightarrow \exp(-2x) \quad \text{for } x \gtrsim 1.5. \tag{43}$$

3.2 Convergence or divergence coefficient

Since it is confirmed from the computations by the use of realistic ionospheric models that the terms $T_c(\nu)$ and $\Delta P(\nu)$ (see eqns. 26 and 25 resp.) appearing in the integrand on the r.h.s. of eqn. 33 can be assumed constant over a significant range of integration at and around $n = z = k_1 a$, the parameter A defined by

$$\text{eqns. 37, 38 and eqn. 41} \rightarrow A = |\Pi_{sk,p}/2\Pi_0| = |BI_p| \quad \text{in which the terms } V_p^-(t) \text{ and } V_p^+(t) \text{ are dropped.}\dagger \tag{44}$$

represents a coefficient replacing

$$\left|\frac{1}{2}C[1+R(\psi)]^2[R(\psi)]^{p-1}\right| \quad (\text{see eqn. 19}) \tag{45}$$

† In the final stage of field-strength prediction of a sky-wave, these functions, i.e., $T(\nu)$ (see eqns. 20, 26, 38) should be replaced by a function representing the effects of 'ionospheric absorption' and polarisation coupling' as is shown in Table 1.

When the propagation takes over a perfectly conducting earth, such as over a sea, and each pair of end-points on the earth's surface and at the bottom of the ionosphere are well intervisible,

$$A = 2C \tag{46}$$

holds exactly.

As is evident from eqns. 44 through 46, the parameter A represents a combined effect of 'terrestrial diffraction' and 'ionospheric convergence' at low to negative angles of departure/arrival. However, for simplicity and from a numerical character exhibited by A, the parameter is defined as the convergence or divergence coefficient. As is also evident from what has been stated above, the problem of estimating A has substantially been reduced to that of propagation in a sapce bounded by a pair of concentric spherical surfaces with radii a and $a+h'$.

3.3 Typical examples of computed A

As a pre-requisite for computing this coefficient, the path geometry of a wave-hop trajectory such as is shown in Fig. 1 should be specified at the outset.

To this end, first, an inhomogeneity of the earth-ionosphere space, which has been

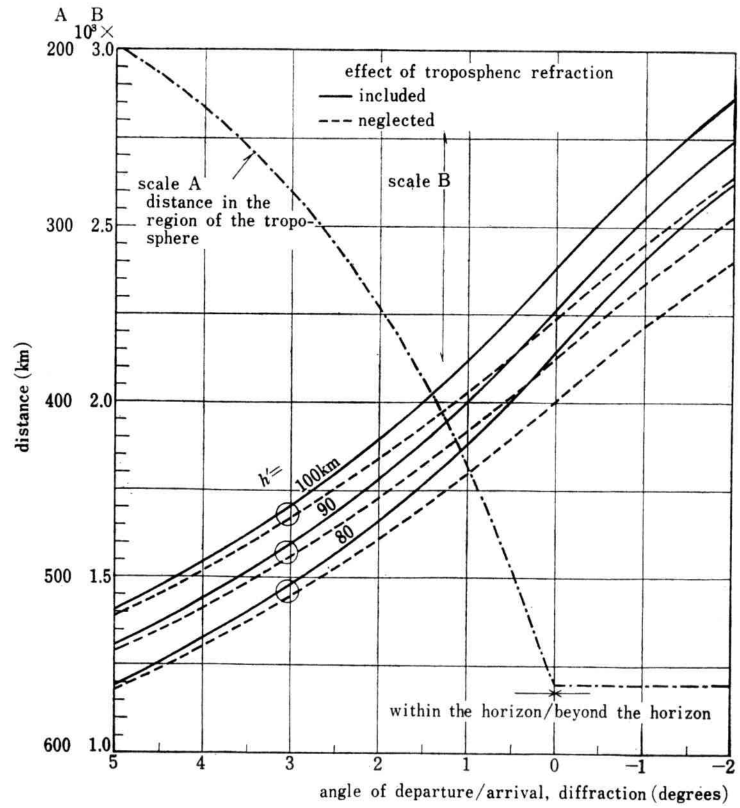

Fig. 3 *Surface distance as a function of angle of departure/arrivalfor a single hop*

represented generally by $k(r)=k_1\mu(r)$ so far, is specialised by modelling the space to a one occupied by a well-known 'basic reference atmosphere'[13] with

$$\mu(r)=[1+300\exp(-0.139h)]10^{-6} \tag{47}$$

where $h=r-a$ is the height (km) above the earth's surface. Obviously eqn. 47 has been introduced to take into account an average effect of the tropospheric refraction on the sky-wave propagation. Secondly, the model of the parabolic ionospheric layer has been specified by fixing the values of the parameters r_1, r_2 and f_p with reference to a number of pieces of work performed by Knight[14] and Wakai[15]. In addition, for the model atmosphere defined by eqn. 47, the value of K appearing in B and in the integral for I_p has been equated to 4/3, and $\mu(r)$ for h exceeding 20 km and up to the bottom of the ionosphere has been equated to unity. The value of 4/3 for K has been derived from a consideration for the average lapse rate of $\mu(r)$ over the height range of first one kilometre. Then the path geometry up to a height of 20 km for a given angle of departure has been determined using eqn. 34 and associated ones, which have been adapted for practical purposes by Bean[13]. On the other hand, the path geometry for the space $20<h<r_1-a$ or $0<h<r_1-a$, the latter applying for a homogeneous earth-ionosphere space, plus the overriding parabolic ionospheric layer has been determined following the method used by Bremmer[2]. Figs. 3a and 3b summarise the above-mentioned geometrical aspects at the range of angles of departure/arrival concerned. These figures show clearly the effects of the tropospheric refraction on the surface distance of a wave-hop path and the angle of incidence at the level of virtual height. In addition, Fig. 3a shows the surface distance, over which a radio-ray traverses the troposphere governed by eqn. 47, as a function of angle of departure/arrival. Once the values of θ and h' have been determined and those of f and p have been fixed, B and I_p given by eqns. 41 and 38, and accordingly A given by eqn. 44, can be determined uniquely. In Figs. 4a and 4b are shown the results of numerical computations of A in term of

$$\text{convergence gain} = 20\log_{10}[A] \quad (dB)$$

at a frequency of 1 MHz for the two typical cases, i.e., the case in the presence of and the one in the absence of the tropospheric refraction, respectively. In these figures, the unbroken or the broken curves apply when all reflection points R_i's fall on a (perfectly conducting) sea ($m=0$) or on a (strongly absorbing) land ($m=p-1$) respectively. The corresponding results at different frequencies show a similar type of traces to those in Figs. 4a and 4b, as may easily be understood from the functional forms of $U_p(t')$ and $f_p(t, \chi, \chi_{h'})$ given by eqns. 41 and 38 respectively. The choice of $h'=90$ km is considered to be most realistic in view of the ionospheric structure given by Wakai[15]. However, it has been confirmed that a choice of different values, 80 km or 100 km, for h' produces an insignificant difference from the results given by Figs. 4*a* and 4*b*.

It is understood from Figs. 4*a* and 4*b*

1) that an infinity catastrophe of the coefficient A at the zero angle of departure/arrival ψ never occurs and a finite value of A is obtained over the full range of ψ even in the absence of a roughness in the ionosphere,

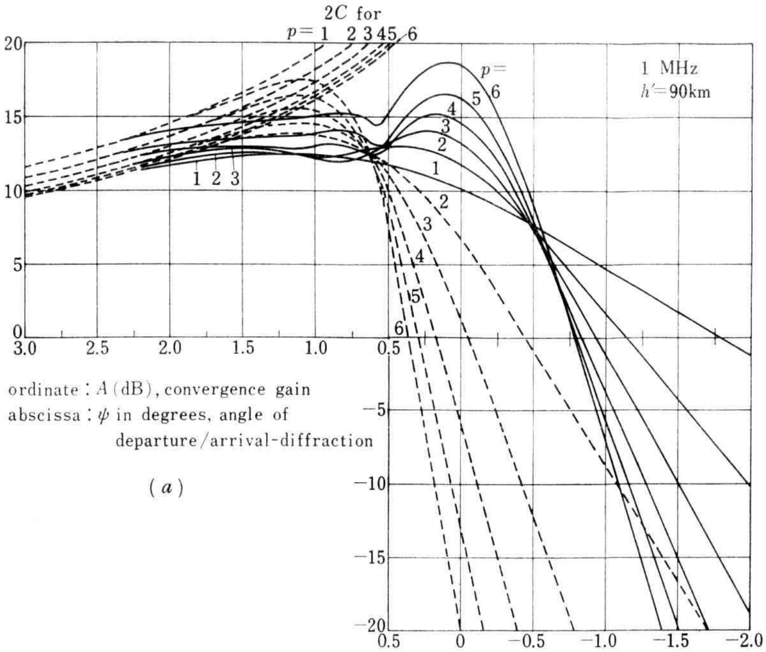

(a)

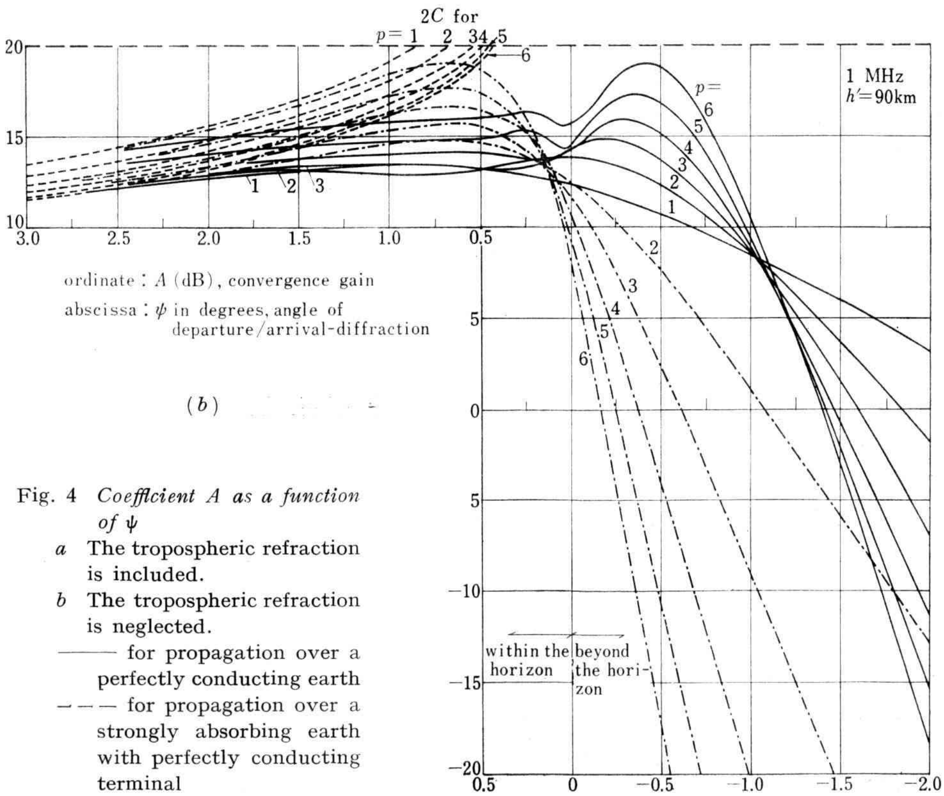

(b)

Fig. 4 *Coefficient A as a function of* ψ

a The tropospheric refraction is included.

b The tropospheric refraction is neglected.

——— for propagation over a perfectly conducting earth

– – – for propagation over a strongly absorbing earth with perfectly conducting terminal

2) that A gradually merges into $2C$ (eqn. 46), which is derived from a simple geometric-optical approach or the second-order approximation for $\Pi_{sk,p}$ referred to in 2.3, when the angles ψ exceed about 2°, independently of the type of ground at and around an intermediate reflection point.
3) that, as the angle of diffraction increases, A is reduced with a progressive rapidity with an increase in the number of hops p.

4. Application of a result of the foregoing analysis to the estimation of interhop polarisation coupling factor

4.1 The ratio Γ_h/Γ_v at low to negative angles of departure/arrival

As is evident from the theoretical basis[8] on which eqn. 2 has been derived, Γ_v and Γ_h allow for a possible modification in amplitude and phase which a vertically polarised (v.p.) and a horizontally polarised (h.p.) components of an e.m. wave may suffer respectively at intermediate ground reflection or diffraction for a pair of adjacent hops. With basis on the highly approximate relation which holds at large distances:

$$E_{sk,p} = k_1^2\, a \cos\psi \cdot \Pi_{sk,p}{}^2 \qquad (a\theta \gg 1) \tag{48}$$

$E_{sk,p}$ being the total field of which vector is in the vertical plane including the 'great circle path', the ratio Γ_h/Γ_v can be derived approximately using a result of the foregoing analysis as follows.

Consider a pair of modes of 'two-hop propagation' with the same type of ground conditions at both terminal points as those employed in Sec. 3, namely 1) the mode in which an e.m. wave is propagated with the vertical polarisation along the full course of the wave-hop path similarly to before, and 2) the mode in which an e.m. wave is propagated with the horizontal polarisation along the intermediate course $T_{i2} \to R_i \to T_{i+1,1}$ (see Fig. 1), but, with the same polarisation as that for the mode 1), along the remaining course. Then the total field for mode 1 is readily obtained from eqns. 33 and 48 as

$$E_1 = E_{sk,p}|_{p=2} \text{ given by eqn. 48, } \Pi_{sk,p}|_{p=2} \text{ itself being given by eqn. 33} \tag{49}$$

The total field for mode 2 can be obtained likewise by the help of eqn. 48. That is to say, the field is obtained formally from the same equation as eqn. 49 only if the factor $N(\xi, K, \delta)/M(\xi, K, \delta)$ appearing on the r.h.s. of eqn. 33 is replaced by $N(\xi, K, \delta_m)/M(\xi, K, \delta_n)$. where δ_m is given by

$$\delta_m = [\delta \text{ in eqn. } 28]/\varepsilon_c \tag{50}$$

δ_m being another parameter introduced by Bremmer[2]. This replacement originates from the use of the spherical reflection coefficient $R_h(\nu)$ at R_i for h.p. in place of $R_v(\nu) = R(\nu)$ given by eqn. 5. Since, at m.f., the approximation $\delta_m = 0$ applies *a fortiori* as compared with the case of reflection of a v.p. wave against a strongly absorbing ground that has been refereed to in Sec. 3.1, the field in question is after all estimated highly approximately by a substituting from eqn. 41 with $p=2$ and $m=1$ into eqn. 38 and a succeeding use of eqns. 37 and 48:

$$E_2 = \Pi_{sk,p}|_{p=2} \text{ given by eqn. 48, } \Pi_{sk,p}|_{p=2} \text{ itself being given by eqns. 41 with } m=1, \text{ 38 and 37} \tag{51}$$

Eqns. 50 and 51 lead to

$$\frac{\Gamma_h}{\Gamma_v} = \frac{E_2}{E_1} \tag{52}$$

Since the factors $T_c(\nu)$ and $\Delta P(\nu)$ appearing in eqns. 33 and 37 can be treated similarly to Sec. 3.2, the ratio Γ_h/Γ_v can also be evaluated in entirely a similar fashion to before.

Although an introduction of two types of propagation modes 1 and 2, the latter mode in particular, is quite artificial, the above-mentioned treatment is justified so far as the estimation of the ratio Γ_h/Γ_v which an e.m. wave may suffer at the intermediate ground reflection or diffraction, is concerned.

When the intermediate reflection or diffraction occurs at a ground, this ratio is highly to reasonably approximated by unity since the parameter δ can then be approximated by zero as has been stated in Sec. 3.1. As a consequence, the most careful examination of the ratio is required for a case in which δ differs greatly from unity, i.e., the intermediate reflection or diffraction occurs at a sea. This case is discussed in the following section.

4.2 Γ_h/Γ_v for the reflection or diffraction at a sea

In this case the parameter δ can be highly approximated by infinity or zero, depending upon the state of polarisation of an e.m. wave, as has been stated in Sec. 3.1 and in the foregoing section. The ratio Γ_h/Γ_v can therefore be readily obtained as part of the result rom the analysis made in Section 3 as follows:

$$\frac{\Gamma_h}{\Gamma_v} = \frac{A|_{p=2,m=1}}{A|_{p=2,m=9}} = \frac{\Pi_{sk,p}|_{p=2,m=1}}{\Pi_{sk,p}|_{p=2,m=0}} \tag{53}$$

where $\Pi_{sk,p}$ being evaluated using eqns. 41, 38 and 37.

Figs. 5a and 5b show typical examples of computed Γ_h/Γ_v in terms of amplitude and phase as a function of angle of departure/arrival in the presence of and in the absence of the effect of tropospheric refraction, respectively.

It is understood from Figs. 5a and 5b

1) that the ratio Γ_h/Γ_v gradually merges into a value -1, which is derived from a simple geometric-optical approach of the second-order approximation for $\Pi_{sk,p}$ referred to in 2.3 as $\Gamma_v = +1$ and $\Gamma_h = -1$, when the angles of departure/arrival ψ exceed about 2°,
2) that, with a decrease in the angles ψ, the ratio tends to deviate progressively from the value -1.

4.3 Inter-hop polarisation coupling factor—relative value F_{rel}

From eqn. 2,

$$F = \Gamma_v^2 \cdot F_{rel}$$

where $$F_{rel} = [\text{the r.h.s. of eqn. 2}]|_{\Gamma_v \to 1,\ \Gamma_h \to \Gamma_h/\Gamma_v} \tag{54}$$

The ratio Γ_h/Γ_v which has been discussed so far enables F_{rel} to be readily evaluated,

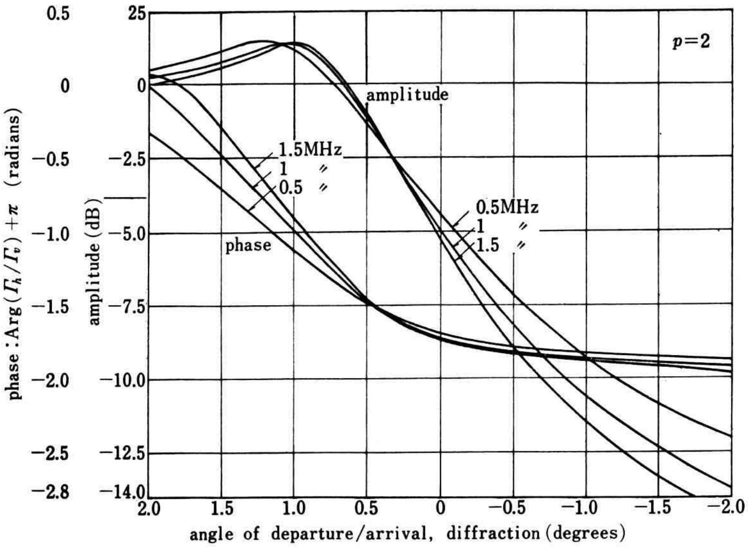

(*a*)

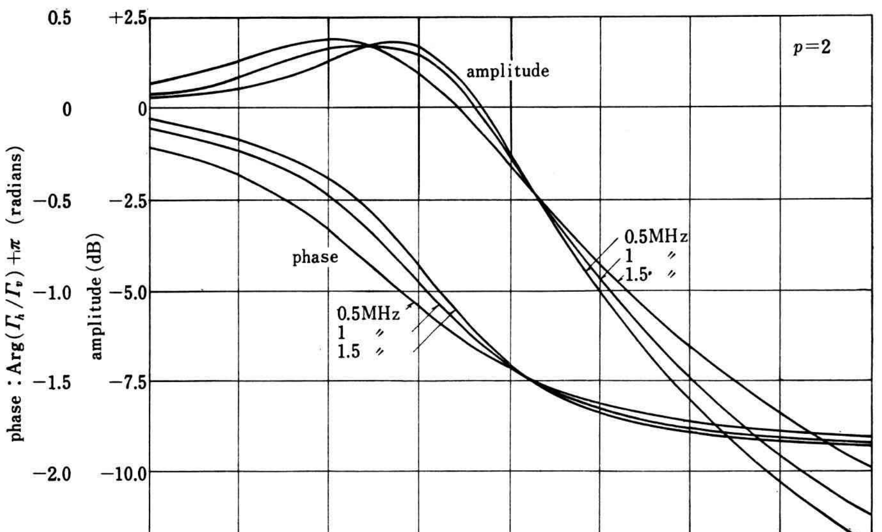

(*b*)

Fig. 5 *Γ_h/Γ_v as a function of ψ*
(*a*) The effect of tropospheric refraction is included.
(*b*) The effect of tropospheric refraction is neglected.

provided that the basic data ionospheric and geomagnetic associated with the parameters $\psi_{a,b}$ and $M_{a,b}$ appearing on the r.h.s. of eqn. 2 are known. To evaluate a true value of F, a full information on Γ_v is needed in addition to that on Γ_h/Γ_v. However, since the value of Γ_v is incorporated in that of $A|_{\delta=\infty}$, i.e., one of the unborken curves given in Fig. 4, as is evident from the analysis made in Sec. 3, a product $A|_{\delta=\infty}\cdot\prod_{i=1}^{p-1} F_{rel}^{1/2}|_i$ enables the effects of overall convergence or diffraction and inter-hop polarisation coupling to be evaluated definitely for the propagation over a perfectly conducting earth, practically such as over a sea. Similarly, with reference to this value the corresponding value for a case in which the propagation does not fully take place over a perfectly conducting earth from the first emergence to the last entry into the ionosphere can be evaluated definitely, no undetermined factor being left in a computed field-strength.

At angles of departure/arrival exceeding about 2°, $\Gamma_h/\Gamma_v=-1$ originates from $\Gamma_v=R_v=+1$ and $\Gamma_h=R_h=-1$ since the geometric-optical approximation for $\Pi_{sk,p}$ applies. As a consequence, $F_{rel}=F$. When the angles are less than about 2° but the intermediate diffraction occurs at a land, $\Gamma_h/\Gamma_v=1$ (Sec. 4.1) may be interpreted to originate from $\Gamma_v=\Gamma_h=R_{v,h}=-1$. In short, under the above-mentioned path conditions the use of the Fresnel reflection coefficients for v.p. and h.p. waves has been confirmed to be justified essentially or at least formally.

On the other hand, when the intermediate diffraction occurs at a sea, the situation is considerably different from the foregoing cases. That is to say, as has been discussed in the previous section, even a formal use of the Frensel reflection coefficients for Γ_v and Γ_h is ruled out at angles of departure/arrival $\psi\lesssim 2°$. Instead, a result such as is shown in Fig. 5 should be used in the computation of F_{rel}.

The most striking feature emerging from the present analysis as a new fact is that, at $\psi\lesssim 1°$, a very small value of F_{rel} or a very large polarisation coupling loss never occurs even when a propagation path is oriented close to or exactly along an N-S direction and in addition the intermediate reflection or diffraction is undergone at a sea. For instance, when the sky-wave propagation takes place exactly along an N-S path, namely the propagation is literally longitudinal, $M_a=M_b=-1$[7] and at $f=1$ MHz, $\psi=0.5°$, Fig. 5a gives

$$\frac{\Gamma_h}{\Gamma_v}=0.866\exp(+j\,1.637\,rad), \tag{55}$$

yielding $F_{rel}=|1+\Gamma_h/\Gamma_v|2/4=0.54=-2.7$ dB.

In contrast to this result, a formal substitution of $\Gamma_v=+1$ and $\Gamma_h=-1$ into eqns. 2 and 54 leads to

$F=F_{rel}=0$, $\therefore$ polarisation coupling loss$=-\infty$ dB,

5. Typical example of application of a result of the present analysis to the prediction of a long-term median field-strength

In Table 1 is summarised a typical example, in which a result of the present analysis has been applied to the prediction of a long-term night-time sky-wave field-strength for Akita-

Table 1 Prediction of median field-strength for Akita-Melbourne path

Geographic location: Transmitting point (Akita) 39°47'N, 139°46'E; Receiving pt. (Melbourne) 37°49'S, 145°12'E Surface distance D_0=8,644.9 km, f=0.770 MHz, Transmitting aerial: 0.424 λ mast radiator, e.r.p.=500 kW. Electrical properties at terminals: κ_e=30, σ=20mS/m (Aki); κ_e=15, σ=1 mS/m (Mel); h'=90 Δm, Δr=10 km, profile of collision frequency $\nu(r)=[4.5-0.35(r-r_1.)]\cdot 10^5$ Hz, magnetic induction B derived from Reference 16; Inverse distance field; $E_I=300/D_0$ mV/m= 30.81 $dB/\ V/m$

Mode (Nr. of hops)		4E				5E			
ψ/ϕ			0.39°/80.5°				2.05°/80.2°		
Column		1	2	3	4	5	6	7	8
Geomag. parameters		$I^{\dagger}$	$\alpha^{\dagger\dagger}$	$f_H{}^{\dagger\dagger\dagger}$	loss	$I^{\dagger}$	$\alpha^{\dagger\dagger}$	$f_H{}^{\dagger\dagger\dagger}$	loss
$-\Lambda$ (dB)					−14.24				−13.82
1st entry		40.71°	179.61°	1.13		43.40°	180.07°	1.16	
	F (dB)				3.22				2.98
1st hop,	F_{abs} (dB)				1.21				1.21
1st to 2–	exit	40.60°	179.59°	1.13		43.30°	180.05°	1.16	
	F_{rel} (dB)				3.58				16.10
nd hop	entry	6.23°	174.68°	0.97	(15.67)	17.81°	176.09°	0.99	(15.38)
2nd hop	F_{abs} (dB)				1.12				1.15
2nd to 3-	exit	6.07°	174.66°	0.97		17.67°	176.03°	0.99	
	F_{rel} (dB)				2.98				16.44
rd hop	entry	−32.27°	171.87°	1.14	(14.11)	−14.01°	172.90°	1.02	(21.17)
3rd hop	F_{abs} (dB)				1.21				1.15
3rd to 4-	exit	−32.40°	171.86°	1.14		−14.16°	172.89°	1.02	
	F_{rel} (dB)				1.70				1.78
th hop	entry	−59.16°	170.67°	1.47		−41.84°	171.46°	1.24	
4th hop	F_{abs} (dB)				1.22				1.22
4th to 5-	exit					−41.95°	171.45°	1.50	
	F_{rel} (dB)								2.45
th hop	entry	—	—	—		−61.31°	170.52°	1.50	
5th hop	F_{abs} (dB)	—	—	—					1.18
Last exit		−59.24°	170.66°	1.47		−61.38°	170.52°	1.50	
	F_{rel} (dB)				0.88				0.74
Rec. pt.	F_{gr} (dB)				20.43				17.69
L_p/D_0 (dB)					0.10				0.11
Total loss (dB)					23.41	(46.63)			50.38 (54.39)
Field-strength (effective value for converted e.r.p. of 1 kW) $(dB/\mu V/m)$	predicted				7.40	(−15.82)			−19.57 (−23.58)
	measured				7.00				7.00

† magnetic dip angle, + and – signs for the north and the south of the magnetic Equator.

†† magnetic bearing of the great-circle path, measured counterclockwise from the Boreal (geographic).

††† gryo-frequency, MHz.

F_{abc} : ionospheric absorption.

F_{gr} : ground loss at receiving oint, rel. loss for $\sigma=\infty$

* during the hours 1430–1530 G.M.T., 1973–1974.

Remark : Bracketed figures represent the values for cases in which Γ_u and Γ_k have been equated to +1 and −1 respectively in eqn. 2.

Melbourne path†. This table, if placed at the end portion of the companion paper (pp. 31-57) by the present author, may be better understood in detail. For the moment, however, by this tabulation it is intended to just demonstrate a profoundly significant role played by the two types of propagation mechanisms, which have been qualitatively discussed in the foregoing sections, in the sky-wave propagation at m.f., along an N-S oversea path and at low angles of departure/arrival in particular. The numerical data of the basic parameters geometrical and physical and the computed results obtained by the use of these data of the individual loss factors are contained in this table. All geomagnetic data were derived with reference to a practical method of IAGA Report[16]. Columns 1 through 4 and 5 through 8 give the results for a case in which the effect of the average effect of tropospheric refraction is allowed for and a case in which the effect is neglected, respectively.

Along the path concerned, the third (4E) and the third and the fourth (5E) intermediate ground reflection points fall on a sea and the remaining ones on a land. Since the angle of departure/arrival is very low for either mode of propagation, the 'convergence gain' A and the 'interhop polarisation coupling loss' F_{rel} were estimated using the methods described in Sections 3 and 4 respectively. The ground constants at and around the intermediate reflection points on land were partly estimated from a geographical consideration in conjunction with the related information furnished from the A.B.C.† The polarisation coupling losses F undergone at the first entry into and the last emergence from the ionosphere were estimated using eqn. 2 of Reference 8, to which eqn. 2 is formally reduced if M_a and ψ_a, or M_b and ψ_b, are equalled zero and Γ_v and Γ_h to unity simultaneously. The ground loss F_{gr} due to diffraction at the receiving point was estimated highly approximately using a formula, which is basically quite the same kind of equation as eqn. 2, but, naturally formulated to meet the physical situation of ground-to-ground propagation and in which a hypothetical transmitting point is situated at T_{p2} in Fig. 1. The same type of loss F_{gt} at the transmitting point can be estimated similarly to before. At a transmitting point, however, in addition to F_{gt} should be considered the effect on the propagation of an electromagnetic property of a radiating system — transmitting aerial, earthening at its base and the nearby ground inclusive, the effect being an important problem in its own right. In the present example, the estimation of F_{gt} was a little bit complicated due to a mixed-path condition on the transmitting side, namely the first 6.4 km land section from the transmitting point is succeeded by a sea. The overall loss caused by all the factors mentioned above was estimated as nearly 0.7 dB. Since an adequacy of this numerical result was well supported by comparison with the measured data, the loss factor concerned was allowed for in the conversion of the value of the e.r.p. By this procedure, the ground section at and around the transmitting point is assumed perfectly conducting, and, accordingly, no ground loss factor is figured out in Table 1. The ionospheric loss F_{abs} due to absorption in the presence of the earth's magnetic field was computed by a step-by-step sum of the integral representing the absorption factor by the use of the basic theory given in Reference 7, but, in a somewhat

† Regular measurements for this path were conducted by Australian Broadcasting Control Board (A.B.C.B.)

simplified fashion as compared with the well-known rigorous method developed by Jones[17]. Further detail concerning the method for estimating F, F_{abs}, and $F_{gr,gt}$ is referred to the companion paper. Instead, in Table 1, attention should be drawn to a difference between a pair of numerical values in non-bracketted, and bracketted gigures, which appear at the bottom of columns 4 and 8, for F_{rel} (dB). to a marked difference betweeen those in column 4 in particular.

As shown in the table, a satisfactory agreement between the predicted and the measured median field-strengths is achieved when the effect of tropospheric refraction is taken into account. The measured median value of 7 dB appearing in the table was obtained as an annual median value from the measurements made during the hours 0330–0430 G.M.T. once a week. As may be readily understood from a comparison between the results tabulated in Columns 4 and 8, 5E-mode produced a very low predicted field-strength even when the effect of tropospheric refraction was allowed for. On the other hand, for a 3E-mode the angle of diffraction is so high that an enhanced diffraction loss makes the contribution from this mode to the total field-strength quite insignificant, whether the tropospheric refraction is present or absent. As a consequence, only the 4E-mode of propagation, or a mode with the possible smallest number of hops allowing for the effect of tropospheric refraction produces the dominant contribution to the field-strength.

Similar results to those that have been mentioned above were obtained for the remaining N-S oversea paths chosen for the A.B.U. field-strength measurement campaign. The foregoing discussion has revealed that, along an N-S multi-hop path fully or mostly over sea, lower inter-hop polarisation coupling losses combined with a higher convergence gain at lower angles of departure/arrival but along a geometric-optically visible path counterbalances a generally increased ground loss at a receiving point. It may be wroth emphasising at this juncture that, although a possible occurrence of an extremely high loss due to an unfavourable inter-hop polarisation coupling along an N-S and S-N paths has been discussed frequently elsewhere, a satisfactory conclusion has not been given, as yet, to an apparent contradiction between the aforesaid high loss and a higher field-strength which has been detected by a number of direct measurements performed extensively so far. In the present analysis, a satisfactory agreement reached in Column 4 of Table 1 is attributed solely to a phase difference considerably deviating from π between the v.p. and the h.p. component waves which have undrgone intermediate ground reflections. This phase difference, in turn, has been obtained in the present example from a consideration for the tropospheric refraction.

6 Conclusion and acknowledgement

The essential features of the combined effects of the terrestrial diffraction and the ionospheric reflection on the night-time m.f. sky-wave propagation at low to negative angles of departure/arrival have been discussed in the foregoing sections, with a practical objective of contributing to the establishment of a prediction method for field-strengths. An

†† Australian Broadcasting Corporation (now Telecom Australia)

adequacy of the present analysis has been demonstrated by a satisfactory agreement between the predicted field-strength incorporating a result from the analysis and the directly measured long-term median field-strength for a typical N-S oversea path.

As has been referred to in the foregoing section, the effect of a given radiating system including that of the ground at and around a transmitting aerial is another problem which requires a sophisticated analysis allowing for a realistic radiation condition. So far as the author is aware, theoretical work on or associated with the subject in question is too much limited as yet. This situation seems to be originating from a number of complexities and varieties involved in the 'radiating system' which is met in practice.

The author would like to take this opportunity to express his hearty gratitude to Dr. N. Wakai, Radio Research Laboratories (RRL, Tokyo), for having provided the author with a great deal of information on the ionospheric structure, and to Dr. H. Hojo, RRL, for having kindly released for author's use his programme for computing the geomagnetic parameters. The author acknowledges the help of late Mr. D.G. Rodoni*, Mr. J.C. Robertson and his colleagues, Telecom Australia, and the staff of the Australian Broadcasting Control Board in their persistent experimental work and the provision of various pieces of useful information pertinent to the propagation paths terminating at Darwin, Brisbane and Melbourne.

References

1) C.C.I.R. Report 431-1: 'Analysis of sky-wave propagation measurements for the frequency range 150 kHz to 1600 kHz', Vol. VI Ionospheric propagation, p. 152 and p. 170 (I.T.U. Geneva, 1974)
2) BREMMER, H.: 'Terrestrial radio waves' (Elsevier, 1949), pp. 153-241
3) MURAKAMI, I.: 'Study on nocturnal propagation characteristics of medium waves', NHK Tech. Journ., 1959, Vol. 11, No. 6, pp. 1-27 (in Japanese)
4) KNIGHT, P.: 'MF propagation: a wave-hop method for ionospheric fieldstrength prediction', B.B.C. Research Department Report 1973/13 (also published in B.B.C. Engineering)
5) C.C.I.R. Report 252-2: 'C.C.I.R. interim method for estimating sky-wave field strength and transmission loss at frequencies between the approximate limits of 2 and 30 MHz', Vol. VI Ionospheric propagation, p. 49 (but the text published separately) (I.T.U. Geneva, 1974)
6) BRADLEY, P.A.: 'Focusing of radio waves reflected from the ionosphere at low angles of elevation', Electronics Letters, June, 1970, Vol. 6, No. 15, pp. 457-458
7) BUDDEN, K.G.: 'Radio waves in the ionosphere' (Cambridge Univ. Press 1961)
8. PHILLIPS, G.J. and KNIGHT, P.: 'Effects of polarisation on a medium-frequency sky-wave service, including the case of multihop paths', Proc. IEE, January, 1965, Vol. 112, No. 1, pp. 31-39
9) WATSON, G.N.: 'A treatise on the theory of Bessel functions' (Cambridge Univ. Press 1922), Chapter VIII Bessel functions of large orders, pp. 225-270
10) JOHLER, J.R. and WALTERS, L.C.: 'On the theory of Low- and Very-Lowradiofrequency waves from the ionosphere', J. Res. NBS-D. Radio Propagation, 1960, Vol. 64D, No. 3, pp. 269-285
11) SHEDDY, C.H.: 'A general analytic solution for reflection from a sharply bounded anisotropic ionosphere', Radio Science, 1968, Vol. 3, No. 8, pp. 792-795

* To the author's profound regret, Mr. Rodoni suddenly passed towards the end of 1977. He was one of the best collaborator to the author in his work of conducting the joint cooperative project of the A.B.U.

12) LANGER, L.E.: 'On the connection formulae and the solutions of the wave equation', Phys. Rev., 1937, Vol. 51, pp. 669–676

13) BEAN, B.R. and Thayer, G.D.: 'Models of the atmospheric radio refractive index', Proc. IRE, 1959, Vol. 47, pp. 740–755
C.C.I.R. Recommendation 369–1: 'Definition of a basic reference atmosphere', Vol. V (I.T.U., Geneva, 1974)

14) KNIGHT, P.: 'M.F. Propagation: Behaviour of the normal ionosphere during the night at sunrise', B.B.C. Research Department Report 1971/22

15) WAKAI, N.: 'Quiet and disturbed structure and variations of the night-time E region', Journ. Geophys. Res., 1967, Vol. 72, No. 17, pp. 4507–4517.
WAKAI, N.: 'Study on the night-time E region and its effects on the radio wave propagation' (reprinted from Journ. of Radio Res. Labs., Tokyo, 1971, Vol. 18, No. 98, pp. 245–348

16) Letter to the editor from the IAGA Working Group: 'The international Geomagnetic Reference Fiedl 1965.0.', Vol. 21, No. 2, Journ. Geomag. and Geoelectricity, May 1969

17) JONES, R.M.: 'A three-dimensional ray tracing computer program', ESSA Tech. Rep., 1966, Inst. for Environmental Research 17-ITSA; Modifications to the three-dimensional ray tracing program described in ESSA 17-ITSA', ESSA Res. Labs., 1968, Inst. for Telecommunication Sciences